

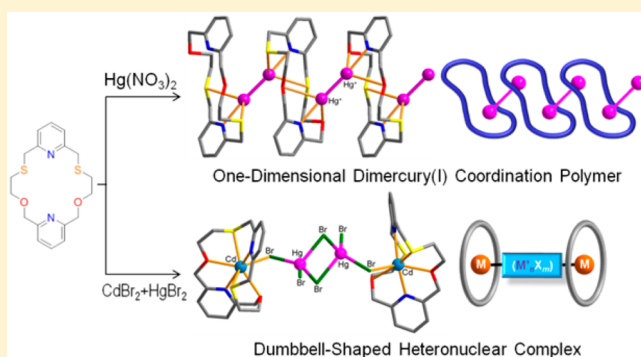
Group 12 Metal Complexes of an 18-Membered N₂O₂S₂ Macrocyclic Ligand Incorporating Two Pyridines: First Examples of an Infinite Mercury(I) Complex and a Dumbbell-Shaped Heteronuclear Complex with a Macrocyclic Ligand

Sujin Seo, Huiyeong Ju, Seulgi Kim, In-Hyeok Park, Eunji Lee,* and Shim Sung Lee*

Department of Chemistry and Research Institute of Natural Sciences, Gyeongsang National University, Jinju 52828, South Korea

Supporting Information

ABSTRACT: Homo- and heteronuclear group 12 metal (Zn²⁺, Cd²⁺, and Hg²⁺) complexes 1–6 containing a newly designed 18-membered N₂O₂S₂ macrocycle incorporating two pyridine subunits (L) were prepared and structurally characterized. The individual complexes isolated exhibit unusual stoichiometries, geometries, oxidation states, and structural topologies and include an infinite mercurous complex and a heteronuclear dumbbell-shaped complex. Both the Zn(II) complex [Zn(L)][ZnBr₄] (1) and the Cd(II) complex [Cd(L)Br₂] (2) are mononuclear, with the metal ion located inside the macrocyclic cavity. The six-coordinated Zn(II) center in 1 adopts an octahedral geometry and is shielded from the anion and solvent by the strongly bound macrocycle. The Cd(II) center in 2 is seven-coordinate, being bound equatorially to two N donors, two O donors, and a S donor from the macrocycle and axially to two bromide ions on opposite sides of the macrocyclic plane, adopting a pentagonal-bipyramidal geometry. In the Hg(II) complexations, the configuration adopted by the macrocycle L shows a dependence of the nuclearity on the anion used. When mercury(II) bromide was used, the dinuclear complex [Hg₂(L)Br₄] (3) was obtained, while the reaction with mercury(II) nitrate afforded the unexpected Hg(I) complex {[Hg₂(L)](NO₃)₂}_n (4) with a one-dimensional polymeric structure. In heterometallic complexation experiments, one-pot reaction of L with a mixture of ZnBr₂ and CdBr₂·4H₂O resulted in the stepwise isolation of two pure solubility-dependent Cd(II) complexes (2 and 5), including the half-dumbbell-type complex [Cd(L)(μ-Br)(CdBr₃)] (5), while a mixture of CdBr₂·4H₂O and HgBr₂ yielded the heterometallic bis(macrocycle) product [(CdL)₂(μ-Hg₂Br₆)](Hg₂Br₆) (6). This is the first example of a heteronuclear dumbbell-shaped complex in which two terminal macrocyclic Cd(II) complexes are linked by a hexabromodimercury(II) cluster via Cd–Br–Hg bonds. The heterometallic dumbbell 6 can be considered as a good example of *competition and collaboration* between Cd(II) and Hg(II) ions because its formation is associated with the higher coordination affinity of Cd(II) toward the macrocycle and the formation of the (Hg₂Br₆)²⁻ cluster, which links the two endocyclic Cd(II) complexes directly. Both NMR titration and comparative NMR data indicate a relatively higher coordination affinity of Cd(II) toward the macrocycle than occurs for Hg(II), in parallel to the situation observed in the solid state.



INTRODUCTION

Macrocyclic complexes with a wide range of structures have been reported over the last four decades.¹ The structural diversity of such complexes often arises from connection of the macrocyclic building blocks via metal centers or coligands using a variety of bridging arrangements.^{2–6} As a result, discrete macrocyclic complexes involve not only 1:1 (metal:ligand) complexes with typical endocyclic complexation but also extended oligomeric analogues such as sandwich,² club sandwich,³ double decker,⁴ cyclic oligomer,⁵ and dumbbell^{6–8} shaped structures displaying unusual stoichiometries.

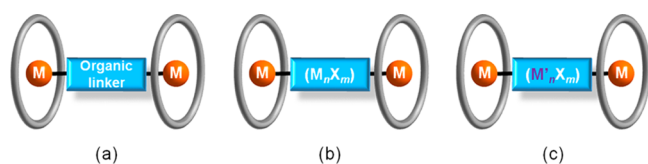
The formation of dumbbells has been achieved by employing two endocyclic complex units and one linker unit (Chart 1).^{6–8} Several macrocyclic dumbbells linked with organic coligands

have been reported by both us⁷ and other groups.⁸ For example, a series of dumbbells of type [(LAG)–L'–(AgL)] in which two endocyclic silver(I)–L complex units are interconnected by organic coligands of type L' [L' = 1,4-diazabicyclo[2.2.2]octane (dabco), 4,4-bipyridine (bpy), or 1,4-bis(4-pyridyl)piperazine (bpp)] have been described.^{7a} A bpy-linked diruthenium(II) dumbbell complex, [{Ru(12S4)–Cl}₂(μ-bpy)] (12S4 = 1,4,7,10-tetrathiacyclododecane), has also been reported by the Grant group.^{8a}

The divalent ions of group 12 metals (Zn, Cd, and Hg) are d¹⁰ systems that cover coordination numbers ranging from 2 to

Received: July 2, 2016

Chart 1. Dumbbell-Shaped Macrocyclic Complexes Linked with (a) Organic Coligands, (b) Homonuclear Clusters, and (c) Heteronuclear Clusters

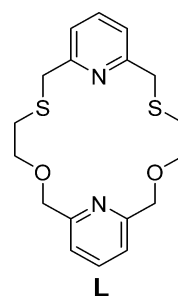


8 with linear to dodecahedral geometries. Unlike its lighter group 12 neighbors zinc and cadmium, mercury commonly exists as a divalent ion but can also exist as the monovalent ion Hg_2^{2+} , which is a dimer via a $\text{Hg}-\text{Hg}$ bond (2.5 Å). Generally, the stability of Hg(I) and the formation of its complexes might be associated with disproportionation to give Hg(0) and Hg(II) . In most mercury complexes, however, the metal centers have a +2 oxidation state because of the lower reactivity and poor purity of the Hg(I) complexes. Only four Hg_2^{2+} complexes of macrocycles have been structurally characterized to date,^{9–12} and thus, the coordination chemistry of Hg(I) complexes with macrocyclic ligands has not been extensively explored.

In our previous work, we found that homonuclear Hg(II) ^{6a} and Cd(II) ^{6b} dumbbells linked by corresponding halide clusters (see Chart 1b) can be formed in one pot-reactions. Our continuing interest in new types of oligomeric macrocyclic complexes prompted us to investigate the possibility of fabricating dumbbell-shaped heteronuclear complexes in which one metal ion (M) is located inside each macrocyclic cavity and a cluster involving another metal ion (M') links the two terminal macrocyclic complex units (see Chart 1c).

Despite their spectroscopically silent nature, the complexation of group 12 metal ions with new ligands has been a popular area of research because of potential biochemical and environmental applications. In general, the coordination chemistry of group 12 metal ions has been conducted using a wide variety of ligand types incorporating N, S, and/or O donors.¹³ In particular, there has been considerable effort directed toward investigating the interaction of group 12 metal ions with various mixed-donor organic ligands, often incorporating pyridyl nitrogen(s) as coordination site(s). The incorporation of versatile pyridine coordination sites into an oxathia macrocycle scaffold may have beneficial effects with respect to coordination mode and stability toward particular metal ions. For example, (i) the endocyclic coordination mode may be favored, (ii) the complex stability may be increased, and (iii) the complexes formed might act as metalloligands for the preparation of oligomeric species.

In this work, we report the synthesis of a ditopic 18-membered macrocycle **L** that provides two different donor sets



associated with its two pyridine domains: the NS_2 donor set approximates a soft-base domain, while the NO_2 donor set approximates a hard-base domain. For both donor sets, the presence of the pyridine N donor is expected to locate inside the cavity. Resulting from our interest in ditopic mixed-donor macrocycles, herein we report the synthesis and structural aspects of **L** bearing two pyridine N donors as well as two S and two O donors, together with its complexation behavior toward group 12 metal ions. In view of the binding affinity to the metal ions with respect to their soft or semisoft base nature, Br^- was selected as a counteranion. In the case of Hg(II) complexations, both Br^- and NO_3^- were employed.

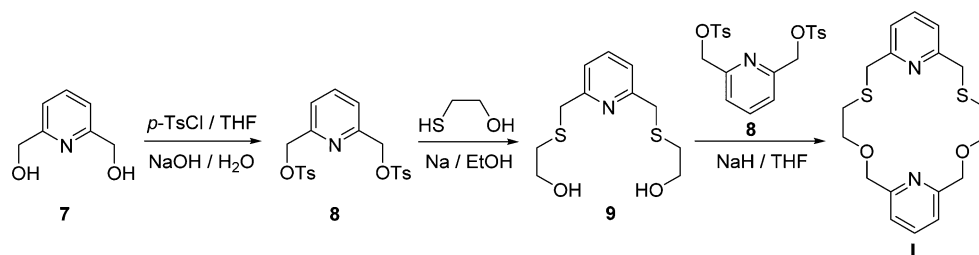
We prepared six complexes (**1–6**) employing the ditopic macrocycle **L**, including one heteronuclear species. As mentioned above, an exciting feature of the results is the formation of a dumbbell-shaped heteronuclear complex. A further intriguing result is the isolation of a Hg(I) complex that shows an infinite structure and forms via Hg(II) reduction. To the best of our knowledge, the observed formation of a dumbbell-shaped heteronuclear complex and a polymeric Hg(I) complex has not been reported previously. Related solution studies including ^1H NMR titrations are also reported.

RESULTS AND DISCUSSION

Synthesis of the $\text{N}_2\text{O}_2\text{S}_2$ Macrocycle **L.** The bimolecular cyclization of dialcohol–ditosylate coupling enables the synthesis of macrocycles via C–O bond formation.^{14a,b} Thus, the target macrocycle **L** was synthesized by a coupling reaction between ditosylate **8** and dialcohol **9** in the presence of sodium hydride in anhydrous tetrahydrofuran (THF) (20% yield; Scheme 1). Compounds **8** and **9** were prepared using known procedures.^{14c,d} The NMR spectra of **L** (Figures S1 and S2) are in accord with its predicted structure.

Zn(II) and Cd(II) Complexes of **L (**1**, $M = \text{Zn}$; **2**, $M = \text{Cd}$).** Both a zinc(II) bromide complex, **1**, and a cadmium(II) bromide complex, **2**, were obtained by reaction of the corresponding metal bromides with **L** in methanol/dichloromethane at room temperature. The yields of the crystalline products were 50–60%. Single-crystal X-ray diffraction (SC-XRD) analysis revealed that both products are mononuclear,

Scheme 1. Synthesis of **L**



with the metal ion located inside the macrocyclic cavity (Figure 1). The Zn(II) complex **1** (Figure 1a) crystallizes in the

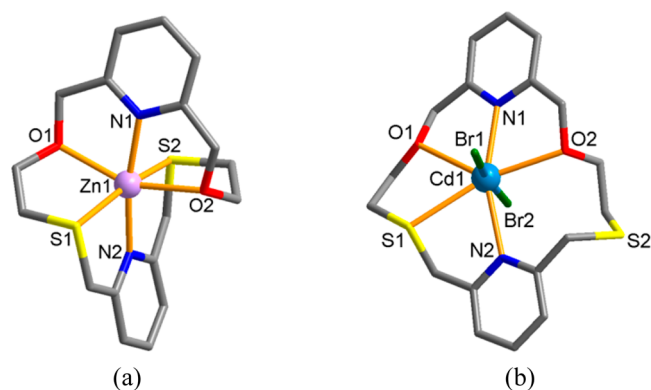


Figure 1. Crystal structures of (a) the zinc(II) bromide complex $[\text{Zn}(\text{L})][\text{ZnBr}_4]$ (**1**) showing a distorted octahedral geometry and (b) the cadmium(II) bromide complex $[\text{Cd}(\text{L})\text{Br}_2]$ (**2**) showing a distorted pentagonal-bipyramidal geometry (also see Figures S3 and S4). The $[\text{ZnBr}_4]^{2-}$ anion in **1** has been omitted.

monoclinic space group $P2_1/n$ with the formula $[\text{Zn}(\text{L})][\text{ZnBr}_4]$; the Cd(II) complex **2** (Figure 1b) also crystallizes in the monoclinic space group $P2_1/n$ but has the formula $[\text{Cd}(\text{L})\text{Br}_2]$. Even though the two complexes share some common features, it is still of interest to compare their structures.

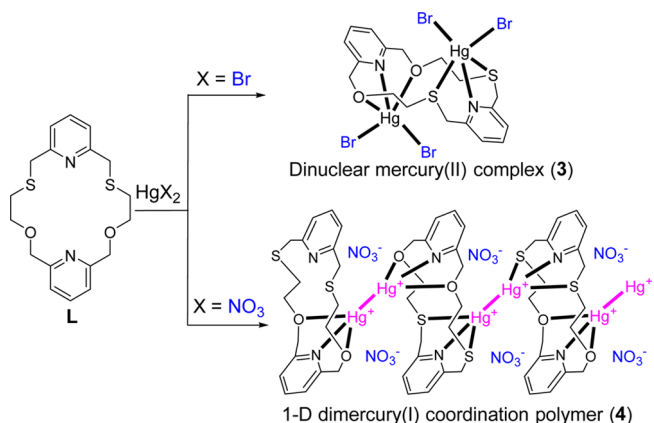
With respect to their coordination geometries, the structural differences between **1** and **2** mainly reflect the effect of anion coordination on the conformational arrangement of **L**. In **1**, for example, the Zn(II) center is six-coordinate, being bound to all of the donors in the macrocycle, which adopts a bent and twisted conformation. The coordination geometry in **1** can be described as a distorted octahedron, with the two O and two S donors from the macrocycle defining the square plane and the axial positions occupied by the two pyridine nitrogen atoms [$\angle\text{N1}-\text{Zn1}-\text{N2} = 169.4(2)^\circ$]. Hence, the metal center in **1** is effectively shielded from the anion and solvent by the bound macrocycle. This preferred anion/solvent-noncoordinated structure in **1** is in keeping with the coordination abilities of the anion and solvent being weaker than that of the macrocycle in this case. In contrast, the Cd(II) center in **2** is seven-coordinate, being bound to two pyridine nitrogen donors, two oxygen donors, and one sulfur donor from the macrocycle as well as two bromide ions on opposite sides of the macrocyclic plane. Thus, the coordination geometry can be described as a distorted pentagonal bipyramid with the five donors of **L** defining the pentagonal plane and the axial positions occupied by the two bromide ions [$\angle\text{Br1}-\text{Cd1}-\text{Br2} = 173.3(2)^\circ$].

Unlike **1**, in **2** one exo-oriented sulfur donor (S2) remains uncoordinated, with a $\text{Cd1}\cdots\text{S2}$ distance of 4.58 Å. As Cd(II) is a soft acid and sulfur is a soft base, it was expected that both sulfur donors (S1 and S2) would bind to the Cd(II) center. This apparently anomalous behavior may be due to the preferred formation of the seven-coordinate geometry and the stronger coordination ability of the Br^- ion toward the Cd(II) center, leading to a puckered conformation of the macrocycle with one sulfur donor uncoordinated. As predicted, the two pyridine nitrogen atoms in **1** bind strongly to the metal center [$\text{Zn1}-\text{N1}$ 2.073(1), $\text{Zn1}-\text{N2}$ 2.115(1)]. In **2**, however, an unexpected longer bond distance for $\text{Cd1}-\text{N2}$ [2.564(2) Å]

over $\text{Cd1}-\text{N1}$ [2.359(2) Å] is observed. The results suggest that hard/soft acid/base (HSAB) considerations with respect to complex formation might be overridden by steric or other geometrical factors associated with complex formation in this case.

Anion-Dependent Mercury Complexes (3 and 4). In the investigation of Hg(II) complexation with **L**, two salts (bromide and nitrate) were used to examine the effect of the anion on the coordination behavior. As shown in Scheme 2, the

Scheme 2. Mercury Complexes with Different Anions



anion dependence is reflected not only in the observed topologies but also in the oxidation states of the metal centers. For example, bromide forms the anion-coordinated discrete dinuclear Hg(II) complex **3**, while nitrate results in the formation of the unprecedented one-dimensional (1D) Hg(I) (Hg_2^{2+}) coordination polymer **4**.

When mercury(II) bromide was reacted with **L** in acetonitrile/dichloromethane, a colorless precipitate was isolated. The precipitate was dissolved in dimethylformamide (DMF), and vapor diffusion of diethyl ether into this solution afforded crystalline **3**. The X-ray crystal structure of **3** shows an interesting dinuclear complex of type $[\text{Hg}_2(\text{L})\text{Br}_4]$ (Figure 2a). Since there is an imposed inversion center present, the asymmetric unit contains one Hg(II) atom, half a molecule of **L**, and two bromide ions. Each Hg(II) center above or below the macrocyclic cavity is five-coordinate, being bound to one pyridine N atom and two O or two S donors in compositional disorder (50:50). The coordination sphere is completed by two bromide ions and adopts a distorted square-pyramidal geometry (Figure 2b), with the three donors from **L** and Br1 forming the square plane while Br2 occupies the apex position. The separation of the two aromatic rings in adjacent macrocycles is inside the range expected for $\pi-\pi$ stacking interactions (centroid-to-centroid distance = 4.00 Å; Figure 2c). Typically, macrocyclic ligands surround one metal ion inside the cavity to form endocyclic mononuclear complexes. However, some larger macrocycles ring sizes greater than 22 atoms sometimes can bind two metal ions in the cavity simultaneously. Our group¹⁵ and other groups¹⁶ have reported dinuclear macrocyclic complexes with 28–40-membered macrocycles synthesized via $[2 + 2]$ cyclization reactions. Some larger Schiff base macrocycles obtained via $[2 + 2]$ cyclization reactions also yield dinuclear complexes.¹⁷ Consequently, the two Hg(II) ions in **3** are located slightly above the chair-shaped macrocyclic plane of **L** to form half-sandwich-type complexes because the cavity is too small to accommodate

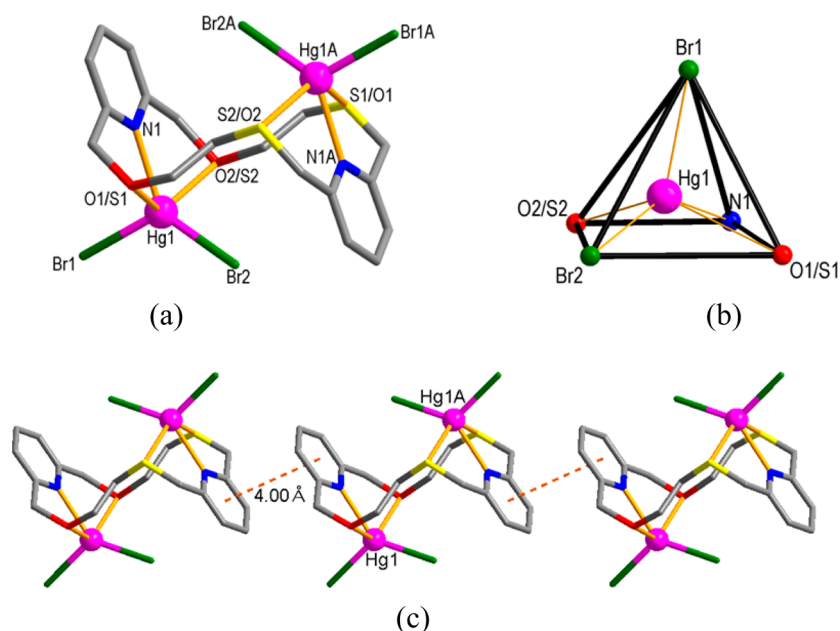


Figure 2. Crystal structure of the mercury(II) bromide complex $[\text{Hg}_2^{\text{II}}(\text{L})\text{Br}_4]$ (3): (a) general view of the dinuclear mercury(II) bromide complex; (b) coordination environment around the Hg1 atom showing a distorted square-pyramidal arrangement; (c) interligand π - π stacking interactions (dashed lines).

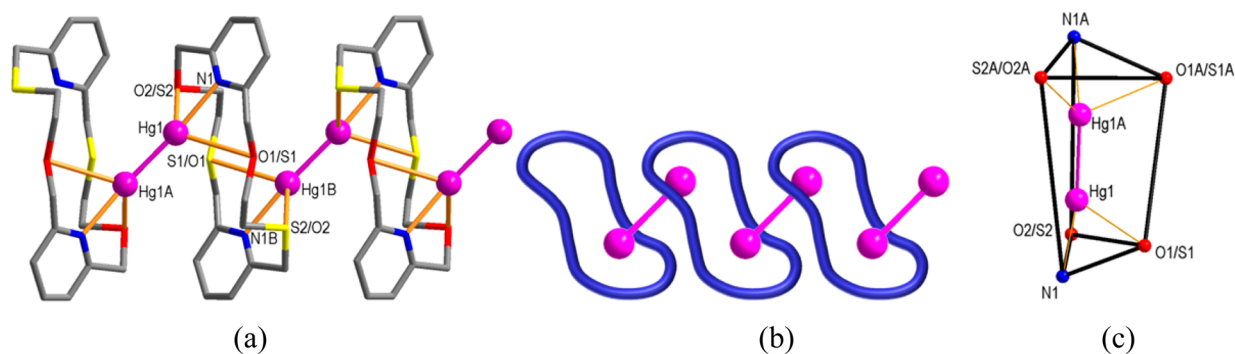


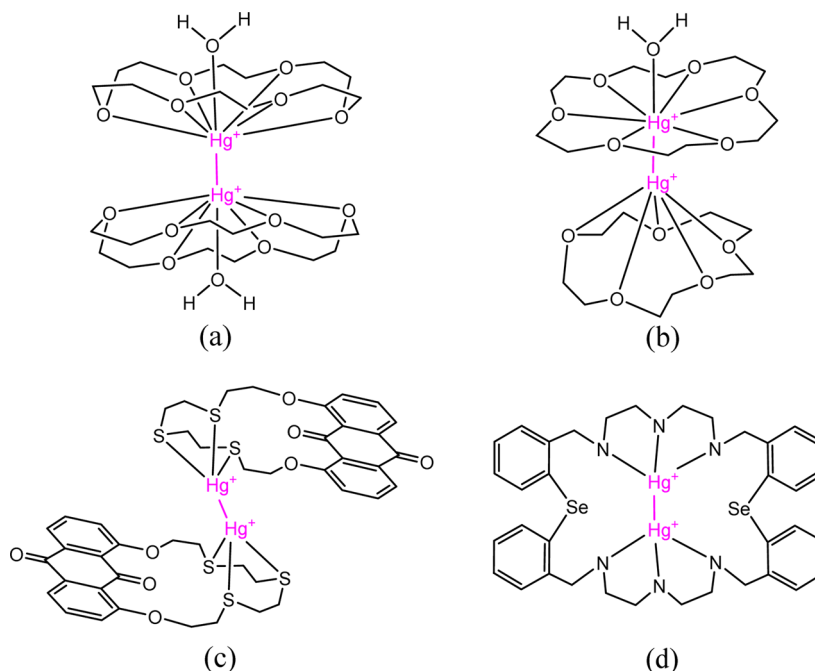
Figure 3. Crystal structure of the mercury(I) nitrate complex $\{[\text{Hg}_2^{\text{I}}(\text{L})](\text{NO}_3)_2\}_n$ (4): (a) 1D polymeric structure linked with dimercury(I) ions ($\text{Hg}^{\text{I}}-\text{Hg}^{\text{I}}$); (b) schematic representation of the 1D linkage; (c) coordination environment around the dimercury(I) ion showing a distorted trigonal-prismatic arrangement. Noncoordinated anions have been omitted.

two metal ions simultaneously. The distance between the two Hg(II) centers is 5.83 Å.

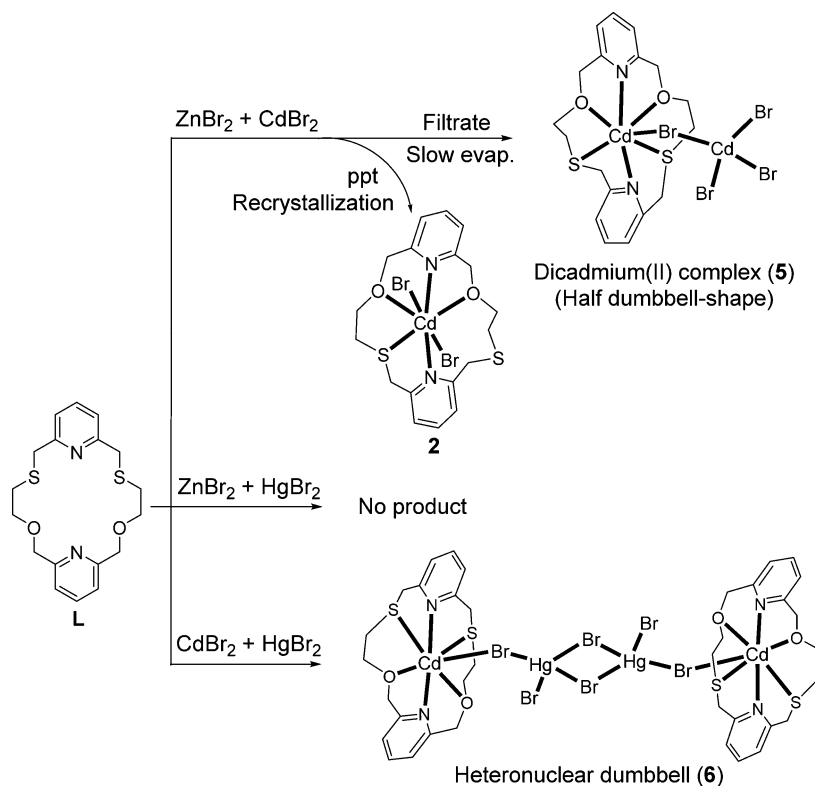
Upon reaction of mercury(II) nitrate with L in acetonitrile/dichloromethane, a colorless precipitate was obtained. According to the elemental analysis and electrospray ionization (ESI) mass spectrum (Figure S7), the reaction produced a mixture of Hg(I) and Hg(II) compounds. Therefore, recrystallization of the impure solid product from DMF/ethyl ether yielded X-ray-quality crystalline 4. The X-ray analysis revealed that 4 is a Hg(I) complex with the formula $\{[\text{Hg}_2^{\text{I}}(\text{L})](\text{NO}_3)_2\}_n$ that adopts an infinite 1D structure in which Hg^+-Hg^+ dimers (Hg_2^{2+}) link the macrocycles, leading to the formation of a polymeric chain (Figure 3a). In 4, the Hg_2^{2+} ions are present on opposite sides of the macrocycle. The Hg1–Hg1A bond distance [2.519(2) Å] is comparable to the corresponding distance in $\text{Hg}_2^{\text{I}}(\text{NO}_3)_2$ [2.508(2) Å]¹² and other reported complexes of this type, showing a 2.49–2.56 Å range,¹⁸ but much shorter than the metallic Hg–Hg distance of 3.00 Å. Again, the two S and two O atoms in L are disordered (50:50). The asymmetric unit in the complex part in 4 contains half of L and one Hg(I) atom. The Hg(I) center coordinates to two

N(O1/S1)(O2/S2) donor sets from two adjacent macrocycles to yield an overall metal coordination geometry of six. The resulting coordination environment of the mercurous dimer ion can be described as a distorted trigonal prism (Figure 3c). The two trigonal faces are defined by N1A–S2A/O2A–O1A/S1A and N1–O1/S1–O2/S2. The macrocycle adopts a twisted and elongated conformation to accommodate two Hg(I) atoms on different sides. The pyridine nitrogen atom also binds strongly to the Hg(I) atom [Hg1–N1 2.294(2) Å]. The nitrate anions in 4 remain uncoordinated, with the closest distance between the Hg and O atoms being 3.0297(2) Å (Figure S5). In this case, no Hg(II) product was recrystallized. As we understand it, complex 4 is the first example of a polymeric Hg(I) macrocyclic complex.

Practically, most of the reported mercury complexes of macrocycles have Hg in the +2 oxidation state. Only four Hg(I) complexes of macrocycles have been reported to date, and all of them have discrete structures (Chart 2).^{9–12} Syntheses of the sandwichlike symmetric $[\text{Hg}_2(18\text{-crown-6})_2(\text{H}_2\text{O})_2]^{2+}$ complex⁹ (Chart 2a) and asymmetric $[\text{Hg}_2(18\text{-crown-6})(15\text{-crown-5})(\text{H}_2\text{O})]^{2+}$ complex¹⁰ (Chart 2b) have been performed

Chart 2. Hg(I) Complexes of Macrocycles Reported Previously^{9–12}

Scheme 3. Complexes Obtained from the Reaction of L with Metal Bromide Mixtures



from a Hg(II) salt over elemental mercury via disproportionation. The Sykes group¹¹ also reported a sandwich-type mercurous complex of 1,8-anthraquinone-18-trithiacrown-5 with the coordination to six sulfur donors from the two macrocycles via the reduction of Hg(II) in DMF (Chart 2c). The Singh group¹² reported a rare complex of a Hg₂²⁺ ion trapped inside a 28-membered N₆Se₂ macrocycle bound

through six nitrogen donors, with the remaining two soft selenium donors being uncoordinated (Chart 2d).

The Baldwin group¹⁹ reported a Hg(I) complex of a tripodal nitrogen ligand isolated from the reaction with a Hg(II) salt via comproportionation of Hg(II) and Hg(0) to give Hg₂²⁺. In a range of studies,²⁰ however, the serendipitous formation of Hg₂²⁺ complexes from Hg(II) has been attributed to the role of the solvent or ligand as the possible reducing agent. Recently,

the Zhang group^{20e} isolated a Hg(I) complex of a pentadentate thioether ligand during an assembly reaction with a Hg(II) salt due to the reductive activity of the thioether ligand used. Therefore, the formation of the Hg(I) complex in this work also seems to be attributed to the reductive activity for the thioether ligand L.

The isolation of **4** in this work is somewhat unusual since mercury(II) nitrate was the preferred metal ion source without addition of elemental mercury as the reductant. In an alternate approach to prepare **4** directly by using mercury(I) nitrate under otherwise identical conditions, a mixture of Hg(I) and Hg(II) products as well as elemental mercury was obtained and confirmed from the ESI-MS and other data (see the elemental mercury in Figure S8 and the ESI-MS spectrum in Figure S9).

Complexation with Mixed Metal Bromides. As an extension of the above homonuclear zinc, cadmium, and mercury complexes, we proceeded to the preparation of the related heteronuclear complexes of L with extended structures, including the dumbbell type. Three possible cases of mixed metal bromides were employed in the reactions with L. As shown in Scheme 3, the reaction of L with Cd/Hg afforded a dumbbell-shaped complex, while Zn/Cd complexation resulted in the isolation of two solubility-dependent Cd(II) complexes with different stoichiometries, including the half-dumbbell-shaped complex **5**. In the case of Zn/Hg, no pure solid product was isolated under the conditions employed.

The reaction of L with a mixture of ZnBr₂ and CdBr₂ afforded two products (**2** and **5**) depending on the separation process. For instance, a colorless precipitate was obtained from the reaction mixture. This was dissolved in DMF, and following ether vapor diffusion, a crystalline product was obtained. X-ray analysis revealed that this product was **2**, which was already obtained via the direct reaction of L with CdBr₂ (see Figure 1b), indicating preferential coordination of Cd(II) over Zn(II). After **2** was separated from the mother liquid, as outlined in Scheme 3, slow evaporation of the filtrate afforded a colorless crystalline product. X-ray analysis confirmed this product to be a new dicadmium(II) complex with the formula [Cd(L)(μ-Br)(CdBr₃)] (**5**) (Figure 4a). Interestingly, **5** is a dinuclear complex in which one macrocyclic monocadmium(II) unit and one CdBr₄²⁻ are linked via a Cd1–Br1 bond [2.696(2) Å], resulting in the formation of the half-dumbbell structure. The endocyclic coordinated Cd1 atom is seven-coordinate, being bound to all six donors from the macrocycle in a twisted conformation; the coordination sphere is completed by one

bromo atom (Br1), resulting in a distorted monocapped trigonal prism geometry (Figure 4b). As mentioned above, complexes **2** and **5** were isolated sequentially from the same reaction flask, and the observed fractional crystallization is due to the lower solubility of **5** than **2**. Once again, Zn(II) is excluded in the formation of **5**, probably due to the higher coordination affinity of L and the anion toward Cd(II) than Zn(II).

Dumbbell-Shaped Heteronuclear [Cd(II)/Hg(II)] Complex **6.** When 1 equiv of HgBr₂ plus 1 equiv of CdBr₂·4H₂O in methanol was used in a one-pot reaction with L in dichloromethane, a colorless crystalline product **6** was obtained. Very interestingly, X-ray analysis revealed that **6** is a dumbbell-shaped heteronuclear complex with the formula [(CdL)₂(μ-Hg₂Br₆)](Hg₂Br₆) (Figure 5a). In **6**, the Cd(II) occupies the cavity of L to form a cationic complex (CdL)²⁺, and two such adjacent cationic units are linked by one anionic hexabromodimercury(II) cluster, (μ-Hg₂Br₆)²⁻, to generate the dumbbell-like bis(macrocyclic) cationic complex [(CdL)₂(μ-Hg₂Br₆)]²⁺. One anionic hexabromodimercury(II) cluster exists separately (see Figure S6). The Cd(II) center is seven-coordinate, being bound to all six donors from L in a twisted conformation, with the remaining coordination site occupied by one bridging Br atom with a Cd1–Br1 distance of 2.769(1) Å, which is slightly longer than the corresponding bond distance found in the half-dumbbell analogue **5** [Cd1–Br1 2.696(1) Å; Figure 4a]. The coordination geometry of the Cd(II) atom is a distorted monocapped trigonal prism, in which one O atom (O2) caps the one distorted rectangular plane (N1–Br1–N2–S2) (Figure 5b). In **6**, the distance between the two Cd(II) centers in the macrocyclic cavities is 11.90 Å.

Previously, our group reported three examples of cluster-linked homonuclear dumbbell-type macrocyclic complexes (Chart 1b): [(CuLCl)₂(μ-CuCl₄)] (L = 18-membered NS₄ macrocycle) (Chart 3a),²¹ [(HgL)₂(μ-Hg₂Br₆)] (L = 20-membered NO₂S₃ macrocycle) (Chart 3b),^{6a} and [(CdL)₂(μ-Cd₄I₁₂)] (L = 20-membered NO₂S₃ macrocycle) (Chart 3c).^{6b} However, our subsequent efforts to prepare heteronuclear dumbbell complexes by employing diverse types of macrocycles, including thiamacrocycles, were not successful. For example, when we employed 1,10-dithia-18-crown-6 (DT18C6) in an attempted assembly reaction with selected metal ion pairs including Cd(II)/Hg(II), a discrete product was obtained with three separated components, namely, [CdI-(DT18C6)]₂[Hg₂I₆] (Chart 3d).²² Thus, **6** obtained in the present work appears to be the first characterized example of an heteronuclear dumbbell complex (Chart 1c) based on a macrocyclic host ligand.

The formation of this heteronuclear dumbbell is more complicated than that for the corresponding homonuclear ones. Thus, the preferred formation of the dumbbell-type heteronuclear species in this work might be considered as a meaningful example of *competition and collaboration* between two group 12 species. In the competition, Cd(II) occupied the macrocyclic cavity over Hg(II), suggesting relatively higher coordination affinity for Cd(II) to the macrocyclic host compared with Hg(II). In the collaboration, the two macrocyclic Cd(II) complex units are linked by Hg(II) via the bridging counterions to generate the heterometallic species via Cd–Br–Hg bonds directly.

NMR Titrations To Investigate Cd(II) and Hg(II) Complexation. For the further understanding of the above

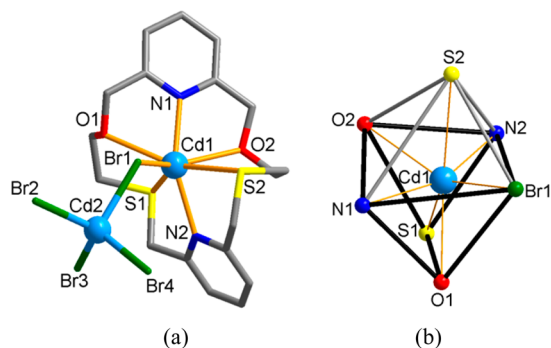


Figure 4. Crystal structure of the dicadmium(II) bromide complex [Cd(L)(μ-Br)(CdBr₃)] (**5**): (a) general view of the half-dumbbell-shaped complex; (b) coordination environment of Cd1 showing a distorted monocapped trigonal prism arrangement.

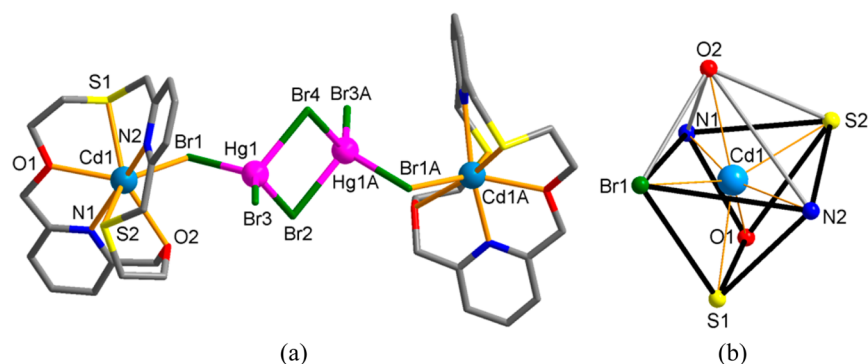


Figure 5. Crystal structure of the heteronuclear Cd(II)/Hg(II) bromide complex $\{[\text{Cd}(\text{L})]_2(\mu\text{-Hg}_2\text{Br}_6)\}[\text{Hg}_2\text{Br}_6]$ (**6**): (a) general view of the dumbbell-shaped bis(macrocycle) complex; (b) coordination environment of Cd1 showing a distorted monocapped trigonal prism arrangement. The separated anionic $[\text{Hg}_2\text{Br}_6]^{2-}$ part has been omitted.

Chart 3

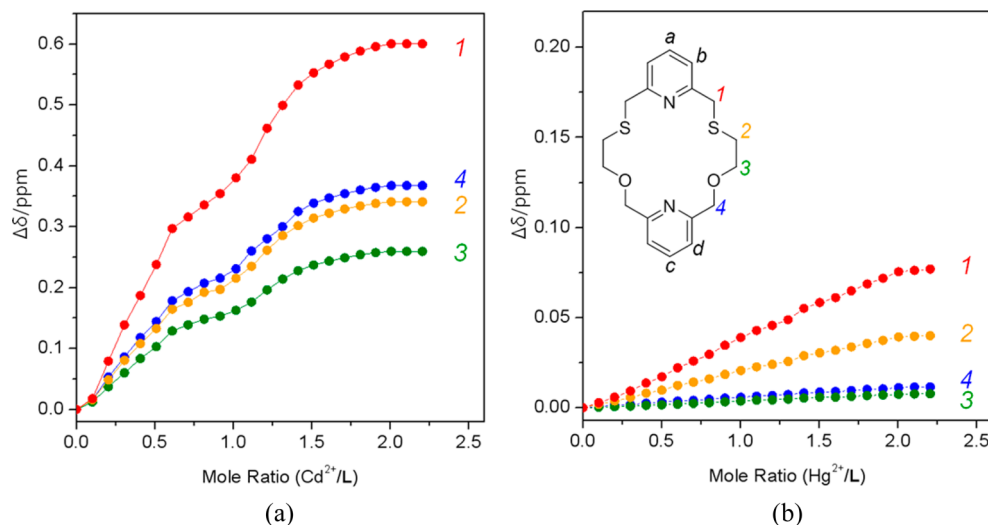
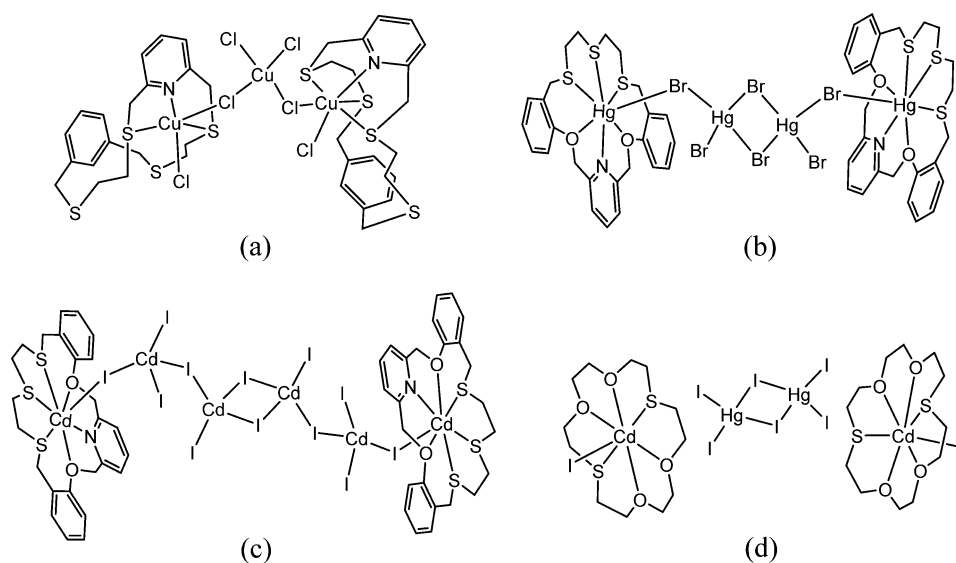


Figure 6. NMR titrations of L with (a) cadmium(II) and (b) mercury(II) (as bromides) in CD_3OD .

heteronuclear dumbbell complex that forms via competition and collaboration between Cd(II) and Hg(II), the corresponding complexation studies in solution were also performed. ^1H NMR titration experiments to follow the interaction of

cadmium(II) bromide and mercury(II) bromide with L were performed in CD_3OD . In both titrations, it was possible to observe the cation-induced chemical shift changes for the macrocycle in which all of the proton resonances shifted

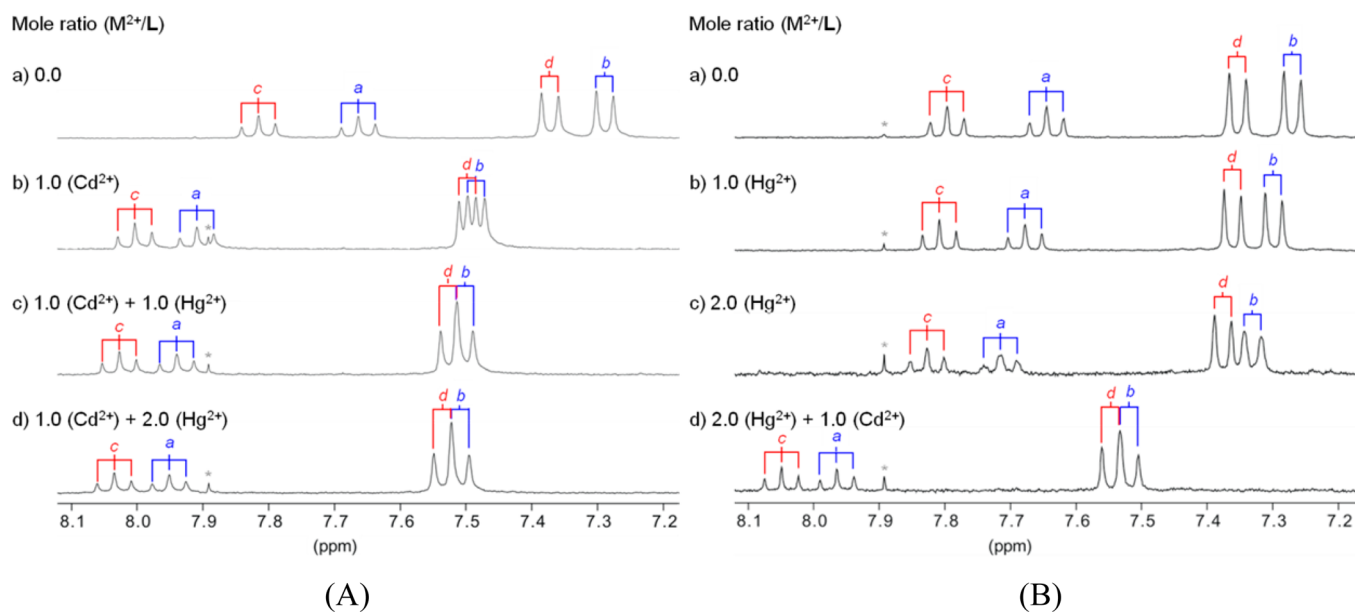


Figure 7. ^1H NMR spectra of the aromatic region for L in CD_3OD via stepwise addition of (A) cadmium(II) followed by mercury(II) (as bromides) or (B) mercury(II) followed by cadmium(II) (as bromides), $[\text{L}] = 3 \text{ mM}$. (C) Proposed complexation equilibria between the corresponding species in solution.

downfield (Figures S10 and S11), indicating complex formation, with the ligand exchange rate being fast on the NMR time scale. The magnitude of the chemical shift change ($\Delta\delta$, ppm) of each resonance peak was measured as a function of the mole ratio (M/L) (Figure 6). The titration curves show that the complexation behaviors of Cd(II) (Figure 6a) and Hg(II) (Figure 6b) are quite different.

The magnitudes of the Cd(II)-induced chemical shift changes for the proton peaks of the macrocycle (0.25–0.60 ppm) are much larger than those for Hg(II) (below 0.08 ppm) without exception. Clearly, this evidence indicates that Cd(II) interacts more strongly with the macrocycle than Hg(II) does in CD_3OD solution. In case of the Cd(II) titration, the complexation process is seen to occur via several steps to give two or more species, including a 1:1 (metal:L) complex, that coexist depending on the mole ratio. In contrast, the Hg(II) titration curves exhibit no significant shifts above a mole ratio of 2.0, indicating the formation of the stable complex with a 2:1 (metal:L) stoichiometry.

In the Cd(II) titration, the complexation-induced shifts follow the order $\text{H}_1 \gg \text{H}_4 > \text{H}_2 > \text{H}_3$ (see Figure 6a for each methylene proton). Notably, the observed largest downfield shift for H_1 between the S donor and the pyridine group is in accord with strong binding of Cd(II) to the S donors, in keeping with the presence of a cooperative effect between Cd–S and Cd–N bonds in solution. The second largest shift was observed for H_4 between the O donor and the pyridine group. The difference between these shifts follows that based on HSAB considerations, as Cd(II) and the S donor are a soft acid and soft base, respectively, but the O donor is a hard base. In the Hg(II) titration, as mentioned above, the Hg(II)-induced chemical shift changes are smaller than those for Cd(II), with the complexation-induced shift changes for the protons, $\text{H}_1 > \text{H}_2 \gg \text{H}_3, \text{H}_4$ differing to some extent from those observed in the Cd(II) titration (Figure 6b). In the Hg(II) case, the $\Delta\delta$ values for H_1 and H_2 are larger than those for H_3 and H_4 , suggesting that Hg(II) is more thiophilic (softer) than Cd(II). In the UV titration for the L–Cd(II) complexation (Figure S12), two isosbestic points (235 and 262 nm) were found to

show the multiple complexation equilibria, similar to the NMR titration results, indicating the existence of several stoichiometric complexed species. However, calculations of the stability constants were impossible with these data because of the large uncertainty.

Comparative NMR Study of Competitive Reactions of Cd(II) and Hg(II) toward L. The relative reactivity of Cd(II) and Hg(II) toward L in solution is a primary issue in the formation of the dumbbell-shaped complex. Therefore, competitive reactions of these two metal ions toward L were investigated by ^1H NMR spectroscopy. The signals of the aromatic protons in the macrocycle (H_a – H_d) are well-resolved and readily identified (see the spectrum given in Figure 7A-a). As shown in Figure 7A-b, the addition of 1.0 equiv of Cd(II) causes downfield shifts for H_a – H_d of 0.15–0.3 ppm and indicates 1:1 complexation with fast ligand exchange occurring on the NMR time scale. In this case, the chemical shift changes for H_a and H_b (marked in blue in Figure 7) near the NS_2 donor domain are larger than those for H_c and H_d (marked in red) near the NO_2 donor domain, indicating that Cd(II) favors binding to the S donors rather than to the O donors. However, further addition of Hg(II) (1.0 or 2.0 equiv) led to no significant chemical shift changes (Figure 7A-c,d), suggesting that the 1:1 Cd(II) complex formed earlier is maintained and no further reaction occurs (as proposed in Figure 7C, clockwise direction).

Comparative NMR experiments for the above competition reaction were also performed in the reverse order of salt addition [i.e., Hg(II) followed by Cd(II)]. As shown in Figure 7B-a,b, the Hg(II) complexation proceeds by two steps. First, the addition of 1.0 equiv of Hg(II) causes downfield shifts for H_a – H_d (0.01–0.03 ppm). Upon addition of another 1.0 equiv of Hg(II), further downfield shifts of each peak were observed (0.02–0.05 ppm), in keeping with the formation of a dimercury(II) species, $[\text{Hg}_2\text{L}]^{4+}$ (Figure 7C). Upon addition of 1.0 equiv of Cd(II), much larger downfield shifts (0.2–0.3 ppm) occur, and the spectral pattern in Figure 7B-d becomes the same as that shown in Figure 7A-d, suggesting that the respective reactions finally reach the formation of the monocadmium(I) species $[\text{CdL}]^{2+}$ (Figure 7C, anticlockwise direction, starting from L). Once again, this result agrees with the titration data, which show that Cd(II) has a higher affinity for L than Hg(II) does. Also, this is in agreement with the results obtained for the solid state.

Similarly, an NMR competition study of Zn(II) and Cd(II) was also performed (Figure S13). As shown in Figure S13A, the addition of 1.0 equiv of Cd(II) caused downfield shifts for all of the aromatic peaks with line broadening. However, further addition of Zn(II) (1–2 equiv) led to no significant chemical shift changes, indicating the higher affinity of L for Cd(II) than Zn(II). The above competition reaction performed in the reverse order of salt addition (Figure S13B) also showed stronger Cd(II) complexation.

In addition, the ^1H NMR spectra of complexes 1, 2, and 3 were added together with that of L in CD_3OD (Figure S14). The peaks of the complexes show general downfield shifts compared with those of free ligand L. In all of the complexes, the induced chemical shift of H_1 (between the pyridine and the sulfur donor) is greater than those of other protons because of the higher affinity of the NS_2 donor set toward the metal center. The order of the magnitudes of the induced chemical shift changes of H_1 for the complexes is Cd (2, 0.24 ppm) > Hg (3, 0.09 ppm) > Zn (1, 0.03 ppm), in accord with Cd(II) being

most strongly bound to L, as found in the competition reactions in solution.

CONCLUSION

The newly designed ditopic macrocycle L was synthesized, and its complexation with group 12 metals was investigated in both the solid and solution states. Both zinc(II) and cadmium(II) bromide complexes feature an endocyclic mononuclear species, but the former adopts an octahedral coordination geometry without anion coordination while the latter yields a pentagonal-bipyramidal geometry with anion coordination at the axial sites. Unlike its smaller neighbors, mercury(II) bromide forms a dinuclear macrocyclic complex. When mercury(II) nitrate was used under the same conditions, an unexpected Hg(I) complex with a one-dimensional polymeric structure was isolated as a first example of such a structure. Mixed metal bromide complexation reactions were also carried out, leading to new heterometallic species. A mixture of ZnBr_2 and $\text{CdBr}_2 \cdot 4\text{H}_2\text{O}$ resulted in the isolation of two Cd(II) complexes with different solubilities, including a half-dumbbell-type monomeric species, while a mixture of $\text{CdBr}_2 \cdot 4\text{H}_2\text{O}$ and HgBr_2 yielded the first example of a heteronuclear dumbbell-type complex in which two macrocyclic Cd(II) complexes are linked by a hexabromodimercury(II) cluster. The isolation of the dumbbell complex 6 provides an elegant example of the role of *competition and collaboration* between Cd(II) and Hg(II) ions in the formation of this unusual heteronuclear complex.

EXPERIMENTAL SECTION

General. All of the chemicals and solvents were of reagent grade and were used without further purification. NMR spectra were recorded on a Bruker 300 spectrometer (300 MHz). The FT-IR spectra were measured with a Nicolet iS10 spectrometer. The ESI mass spectra were obtained on a Thermo Scientific LCQ Fleet spectrometer. Elemental analyses were carried out on a Thermo Scientific Flash 2000 series elemental analyzer.

Synthesis and Characterization of L. The precursor diol 9 (1.00 g, 3.87 mmol) was dissolved in anhydrous THF (15 mL), and the solution was added dropwise to a stirred suspension of NaH (0.23 g, 9.67 mmol) in anhydrous THF (15 mL) under nitrogen. After addition of the diol at room temperature, the mixture was refluxed for 1 h and then cooled to 0 °C. 2,6-Bis(tosyloxymethyl)pyridine (8) (1.73 g, 3.87 mmol) was dissolved in anhydrous THF (30 mL), and the solution was added slowly dropwise to the reaction mixture. The reaction mixture was stirred rapidly for 48 h at room temperature and then evaporated. The residue was partitioned between water and dichloromethane. The aqueous phase was separated and extracted with two further portions of dichloromethane. The combined organic phases were dried with anhydrous sodium sulfate and then evaporated to dryness. Flash column chromatography (SiO_2 ; 3:7 dichloromethane/ethyl acetate) afforded the product as a white solid in 35% yield. Mp: 86–87 °C. ^1H NMR (300 MHz, CDCl_3): δ 7.69 (t, 1H, Ar), 7.59 (t, 1H, Ar), 7.28 (d, 2H, Ar), 7.23 (d, 2H, Ar), 4.66 (s, 4H, ArCH_2O), 3.78 (s, 4H, ArCH_2S), 3.71 (t, 4H, $\text{SCH}_2\text{CH}_2\text{O}$), 2.68 (t, 4H, $\text{SCH}_2\text{CH}_2\text{O}$). ^{13}C NMR (75 MHz, CDCl_3): δ 158.19, 157.69, 137.61, 137.23, 121.40, 120.97, 73.39, 69.50, 37.47, 30.28. IR (KBr pellet): 3058, 2912, 2865, 1585, 1451, 1358, 1285, 1221, 1153, 1082, 1027, 989, 934, 831, 815, 756, 724, 696 cm^{-1} . Anal. Calcd for $[\text{C}_{18}\text{H}_{22}\text{N}_2\text{O}_2\text{S}_2]$: C, 59.64; H, 6.12; N, 7.73; S, 17.69%. Found: C, 59.73; H, 6.17; N, 7.40; S, 17.33%. Mass spectrum (ESI): m/z 363.20 $[\text{L}]^+$.

Preparation of $[\text{Zn}(\text{L})][\text{ZnBr}_4]$ (1). Zinc(II) bromide (9.4 mg, 0.042 mmol) in methanol (1 mL) was added to a solution of L (10.1 mg, 0.028 mmol) in dichloromethane (1 mL). Slow evaporation of the solution afforded 1 as a colorless crystalline product suitable for X-ray analysis. Mp: 224–225 °C (decomp.) IR (KBr pellet): 3058, 3027,

2920, 2889, 1656, 1600, 1573, 1545, 1457, 1408, 1360, 1291, 1188, 1163, 1045, 1022, 951, 930, 803, 701 cm^{-1} . Anal. Calcd for $[\text{C}_{18}\text{H}_{22}\text{Zn}_2\text{Br}_4\text{N}_2\text{O}_2\text{S}_2]$: C, 26.60; H, 2.73; N, 3.45; S, 7.89%. Found: C, 26.68; H, 2.73; N, 3.35; S, 7.99%. Mass spectrum (ESI): m/z 214.08 $[\text{Zn}(\text{L})]^{2+}$.

Preparation of $[\text{Cd}(\text{L})\text{Br}_2]$ (2). In a glass tube, $\text{CdBr}_2 \cdot 4\text{H}_2\text{O}$ (14.2 mg, 0.041 mmol) in methanol (1 mL) was layered onto a solution of L (10.1 mg, 0.028 mmol) in dichloromethane (1 mL), and 2 was obtained as an X-ray-quality colorless crystalline product. Mp: 229–230 °C (decomp.). IR (KBr pellet): 3064, 2921, 2863, 1655, 1599, 1455, 1420, 1368, 1293, 1169, 1086, 1003, 806, 756, 660 cm^{-1} . Anal. Calcd for $[\text{C}_{18}\text{H}_{22}\text{CdBr}_2\text{N}_2\text{O}_2\text{S}_2]$: C, 34.06; H, 3.49; N, 4.41; S, 10.10%. Found: C, 34.13; H, 3.48; N, 4.53; S, 10.30%. Mass spectrum (ESI): m/z 555.00 $[\text{Cd}(\text{L})\text{Br}]^+$.

Preparation of $[\text{Hg}^{\text{II}}(\text{L})\text{Br}_4]$ (3). Mercury(II) bromide (14.9 mg, 0.041 mmol) in acetonitrile (1 mL) was added to a solution of L (10.1 mg, 0.028 mmol) in dichloromethane (1 mL). The colorless precipitate obtained was filtered and dissolved in DMF. Vapor diffusion of diethyl ether into the DMF solution afforded 3 as a colorless crystalline product suitable for X-ray analysis. Mp: 182–183 °C (decomp.). IR (KBr pellet): 3067, 2924, 1743, 1653, 1598, 1575, 1452, 1398, 1369, 1238, 1166, 1078, 1005, 805, 757, 674 cm^{-1} . Anal. Calcd for $[\text{C}_{18}\text{H}_{22}\text{Hg}_2\text{Br}_4\text{N}_2\text{O}_2\text{S}_2]$: C, 19.96; H, 2.05; N, 2.59; S, 5.92%. Found: C, 20.37; H, 2.04; N, 2.58; S, 5.99%. Mass spectrum (ESI): m/z 643.17 $[\text{Hg}^{\text{II}}(\text{L})\text{Br}]^+$, 282.25 $[\text{Hg}^{\text{II}}(\text{L})]^{2+}$.

Preparation of $[\{\text{Hg}^{\text{II}}(\text{L})\}(\text{NO}_3)_2]_n$ (4). $\text{Hg}(\text{NO}_3)_2 \cdot \text{H}_2\text{O}$ (14.2 mg, 0.041 mmol) in acetonitrile (1 mL) was added to a solution of L (10.2 mg, 0.028 mmol) in dichloromethane (1 mL). A colorless precipitate was formed in 60% yield after 1 h of stirring. The precipitate was filtered off, washed with diethyl ether, and dried in air. For the further purification, the precipitate was dissolved in DMF and filtered to remove the insoluble impurity. Vapor diffusion of diethyl ether into the DMF solution afforded 4 as a colorless crystalline product suitable for X-ray analysis. Yield: 20%. Mp: 141–142 °C. IR (KBr pellet): 3022, 2922, 2860, 1599, 1578, 1480, 1440, 1383, 1301, 1133, 1106, 1088, 1033, 1004, 933, 813, 791, 710 cm^{-1} . Anal. Calcd for $[\text{C}_{18}\text{H}_{22}\text{Hg}_2\text{N}_4\text{O}_8\text{S}_2] \cdot \text{H}_2\text{O} \cdot \text{CH}_3\text{CN}$: C, 25.37; H, 2.87; N, 7.40%. Found: C, 25.08; H, 2.61; N, 7.42%.

Preparation of $[\text{Cd}(\text{L})(\mu\text{-Br})(\text{CdBr}_3)]$ (5). A mixture of zinc(II) bromide (9.4 mg, 0.042 mmol) and cadmium(II) bromide (14.4 mg, 0.042 mmol) in methanol (1 mL) was added to a solution of L (10.2 mg, 0.028 mmol) in dichloromethane (1 mL). A colorless precipitate formed after 1 h of stirring was isolated by filtration (40% yield). The precipitate was recrystallized by dissolution in DMF followed by vapor diffusion of diethyl ether to afford single crystals that were confirmed by SC-XRD to be compound 2. From slow evaporation of the filtrate for 2 days, the colorless crystalline product 5 was obtained. Mp: 220–221 °C (decomp.). IR (KBr pellet): 2923, 2854, 1657, 1601, 1575, 1546, 1453, 1418, 1367, 1284, 1258, 1163, 1084, 1046, 1010, 807, 790, 736 cm^{-1} . Anal. Calcd for $[\text{C}_{18}\text{H}_{22}\text{Cd}_2\text{Br}_4\text{N}_2\text{O}_2\text{S}_2]$: C, 23.84; H, 2.44; N, 3.09; S, 7.07%. Found: C, 23.94; H, 2.45; N, 3.05; S, 6.98%. Mass spectrum (ESI): m/z 238.17 $[\text{Cd}(\text{L})]^{2+}$, 555.17 $[\text{Cd}(\text{L})\text{Br}]^+$.

Preparation of $[\{\text{Cd}(\text{L})_2(\mu\text{-Hg}_2\text{Br}_6)\}(\text{Hg}_2\text{Br}_6)]$ (6). $\text{CdBr}_2 \cdot 4\text{H}_2\text{O}$ (28.5 mg, 0.083 mmol) and mercury(II) bromide (30.1 mg, 0.083 mmol) in methanol (1 mL) were layered onto a solution of L (10.2 mg, 0.028 mmol) in dichloromethane (1 mL), and 6 was obtained as an X-ray-quality colorless crystalline product. Mp: 189–190 °C (decomp.). IR (KBr pellet): 3068, 2923, 2876, 1601, 1574, 1451, 1406, 1364, 1283, 1239, 1195, 1164, 1085, 1049, 1009, 880, 791, 736, 671 cm^{-1} . Anal. Calcd for $[\text{C}_{18}\text{H}_{22}\text{Cd}_4\text{Hg}_2\text{Br}_6\text{N}_2\text{O}_2\text{S}_2]$: C, 15.95; H, 1.64; N, 2.07%. Found: C, 16.07; H, 1.90; N, 2.23%. Mass spectrum (ESI): m/z 555.08 $[\text{Cd}(\text{L})\text{Br}]^+$, 643.17 $[\text{Hg}^{\text{II}}(\text{L})\text{Br}]^+$.

X-ray Crystallographic Analysis. All of the data were collected on a Bruker SMART APEX II ULTRA diffractometer equipped with graphite monochromatized Mo $\text{K}\alpha$ radiation ($\lambda = 0.71073$ Å) generated by a rotating anode. The cell parameters for the compounds were obtained from least-squares refinement of the spot (from 36 collected frames). Data collection, data reduction, and semiempirical absorption corrections were carried out using the APEX2 software package.²³ All of the calculations for the structure determination were

carried out using the SHELXTL package.²⁴ In all cases, all non-hydrogen atoms were refined anisotropically and all hydrogen atoms were placed in idealized positions and refined isotropically in a riding manner along with their respective parent atoms. Relevant crystal data collection and refinement data for the crystal structures of 1–6 are summarized in Table S1.

■ ASSOCIATED CONTENT

Supporting Information

The Supporting Information is available free of charge on the ACS Publications website at DOI: 10.1021/acs.inorgchem.6b01583.

NMR spectra, additional crystal structures, ESI-MS spectra, NMR titrations, and crystal data (PDF)
Crystallographic data for 1–6 (CIF)

■ AUTHOR INFORMATION

Corresponding Authors

*E-mail: rubiyi7@naver.com.

*E-mail: sslee@gnu.ac.kr.

Notes

The authors declare no competing financial interest.

■ ACKNOWLEDGMENTS

This work was supported by the NRF (2012R1A4A1027750), South Korea.

■ REFERENCES

- (1) (a) Alexander, V. Design and Synthesis of Macrocyclic Ligands and Their Complexes of Lanthanides and Actinides. *Chem. Rev.* **1995**, *95*, 273–342. (b) Radecka-Paryzek, W.; Patroniak, V.; Lisowski, J. Metal Complexes of Polyaza and Polyoxaza Schiff Base Macrocycles. *Coord. Chem. Rev.* **2005**, *249*, 2156–2175. (c) Love, J. B. A Macrocyclic Approach to Transition Metal and Uranyl Pacman Complexes. *Chem. Commun.* **2009**, *22*, 3154–3165. (d) Lindoy, L. F. *The Chemistry of Macrocyclic Complexes*; Cambridge University Press: Cambridge, U.K., 1989. (e) Lehn, J.-M. *Supramolecular Chemistry: Concepts and Perspectives*; VCH: Weinheim, Germany, 1995. (f) Izatt, R. M.; Pawlak, K.; Bradshaw, J. S.; Bruening, R. L. Thermodynamic and Kinetic Data for Macrocyclic Interaction with Cations, Anions, and Neutral Molecules. *Chem. Rev.* **1995**, *95*, 2529–2586. (g) Christensen, J. J.; Eatough, D. J.; Izatt, R. M. The Synthesis and Ion Bindings of Synthetic Multidentate Macrocyclic Compounds. *Chem. Rev.* **1974**, *74*, 351–384.
- (2) (a) Pedersen, C. J. Crystalline Salt Complexes of Macrocyclic Polyethers. *J. Am. Chem. Soc.* **1970**, *92*, 386–391. (b) Seo, J.; Song, M. R.; Lee, J.-E.; Lee, S. Y.; Yoon, I.; Park, K.-M.; Kim, J.; Jung, J. H.; Park, S. B.; Lee, S. S. Exo-Coordination-Based Supramolecular Silver(I) Complexes of S_2O Macrocycles: Effect of Ligand Isomerism on the Structural Diversity. *Inorg. Chem.* **2006**, *45*, 952–954. (c) Yoon, I.; Seo, J.; Lee, J.-E.; Song, M. R.; Lee, S. Y.; Choi, K. S.; Jung, O.-S.; Park, K.-M.; Lee, S. S. Donor Effect on Supramolecular Structures of Silver(I) Perchlorate Complexes of Macrocycles with $\text{O}_2\text{S}_2\text{X}$ ($\text{X} = \text{S}, \text{O}$ and NH) Donor Sets. *Dalton Trans.* **2005**, 2352–2354. (d) Park, S.; Lee, S. Y.; Lee, S. S. Discrete Mercury(II) Complexes, One-Dimensional and Palladium(II)-Mediated Two-Dimensional Silver(I) Coordination Polymers of NS_2 -Macrocyclic: Synthesis and Structural Characterization. *Inorg. Chem.* **2010**, *49*, 1238–1244. (e) Jo, M.; Seo, J.; Seo, M. L.; Choi, K. S.; Cha, S. K.; Lindoy, L. F.; Lee, S. S. Donor-Set-Induced Coordination Sphere and Oxidation-State Switching in the Copper Complexes of $\text{O}_2\text{S}_2\text{X}$ ($\text{X} = \text{S}, \text{O}$ and NH) Macrocycles. *Inorg. Chem.* **2009**, *48*, 8186–8191. (f) Lee, S.-G.; Park, K.-M.; Habata, Y.; Lee, S. S. Endo- and Exocyclic Supramolecular Complexes of Mixed-Donor Macrocycles via [1:1] and [2:2] Cyclizations. *Inorg. Chem.* **2013**, *52*, 8416–8426. (g) Siewe, A. D.; Ju, H.; Lee, S. S. Preparation and Crystal Structures of Silver(I), Mercury(II), and

- Lead(II) Complexes of Oxathia-Tribenzo-Macrocycles. *Bull. Korean Chem. Soc.* **2013**, *34*, 725–730. (h) Beattie, C.; Farina, P.; Levason, W.; Reid, G. Oxa-thia-, Oxa-Selena and Crown Ether Macrocylic Complexes of Tin(II) Tetrafluoroborate and Hexafluorophosphate-Synthesis, Properties and Structures. *Dalton Trans.* **2013**, *42*, 15183–15190.
- (3) (a) Lee, S. Y.; Park, S.; Lee, S. S. Copper(I), Silver(I), and Palladium(II) Complexes of a Thioxamacrocycle Displaying Unusual Topologies. *Inorg. Chem.* **2009**, *48*, 11335–11341. (b) Seo, J.; Song, M. R.; Lee, J.-E.; Lee, S. Y.; Yoon, I.; Park, K.-M.; Kim, J.; Jung, J. H.; Park, S. B.; Lee, S. S. Exo-Coordination-Based Supramolecular Silver(I) Complexes of S₂O Macrocycles: Effect of Ligand Isomerism on the Structural Diversity. *Inorg. Chem.* **2006**, *45*, 952–954. (c) Park, I.-H.; Park, K.-M.; Lee, S. S. Preparation and Characterization of Divalent Hard and Soft Metal (M = Ca, Co, Cu, Zn, Cd, Hg and Pb) Complexes of 1,10-Dithia-18-Crown-6: Structural Versatility. *Dalton Trans.* **2010**, *39*, 9696–9704. (d) Kim, J.; Shamsipur, M.; Huang, S. Z.; Huang, R. H.; Dye, J. L. Sandwich and Mixed Sandwich Complexes of the Cesium Ion with Crown Ethers in Nitromethane. *J. Phys. Chem. A* **1999**, *103*, 5615–5620.
- (4) (a) Kang, Y.; Park, I.-H.; Ikeda, M.; Habata, Y.; Lee, S. S. A Double Decker Type Complex: Copper(I) Iodide Complexation with Mixed Donor Macrocycles via [1:1] and [2:2] Cyclisations. *Dalton Trans.* **2016**, *45*, 4528–4533. (b) Sarnicka, A.; Starynowicz, P.; Lisowski, J. Controlling the Macrocycle Size by the Stoichiometry of the Applied Template Ion. *Chem. Commun.* **2012**, *48*, 2237–2239. (c) Cao, W.; Wang, H.; Wang, X.; Lee, H. K.; Ng, D. K. P.; Jiang, J. Constructing Sandwich-Type Rare Earth Double-Decker Complexes with N-Confused Porphyrinato and Phthalocyaninato Ligands. *Inorg. Chem.* **2012**, *51*, 9265–9272. (d) Berlicka, A.; Latos-Grażyński, L. Intramolecular Rotation of Iron(II) Dithiaethyneporphyrin Double-Decker Complex: ¹H NMR Studies. *Inorg. Chem.* **2009**, *48*, 7922–7930. (e) Kubiak, R.; Janczak, J. Structural and Spectroscopic Characterization of the Holmium Double-Decker Partially Oxidized and Bi-Radical Phthalocyanine Complexes with Iodine. *Inorg. Chim. Acta* **2010**, *363*, 2461–2466. (f) Zhang, X.; Muranaka, A.; Lv, W.; Zhang, Y.; Bian, Y.; Jiang, J.; Kobayashi, N. Optically Active Mixed Phthalocyaninato-Porphyrinato Rare-Earth Double-Decker Complexes: Synthesis, Spectroscopy, and Solvent-Dependent Molecular Conformations. *Chem. - Eur. J.* **2008**, *14*, 4667–4674. (g) Jiang, J.; Bian, Y.; Furuya, F.; Liu, W.; Choi, M. T. M.; Kobayashi, N.; Li, H.-W.; Yang, Q.; Mak, T. C. W.; Ng, D. K. P. Synthesis, Structure, Spectroscopic Properties, and Electrochemistry of Rare Earth Sandwich Compounds with Mixed 2,3-Naphthalocyaninato and Octaethylporphyrinato Ligands. *Chem. - Eur. J.* **2001**, *7*, 5059–5069.
- (5) (a) Lee, E.; Lee, S. Y.; Lindoy, L. F.; Lee, S. S. Metallacycles Derived from Metal Complexes of Exo-Coordinated Macrocylic Ligands. *Coord. Chem. Rev.* **2013**, *257*, 3125–3138. (b) Lee, S. Y.; Seo, J.; Yoon, I.; Kim, C.-S.; Choi, K. S.; Kim, J. S.; Lee, S. S. A Poly(bicyclic dimer) and a Cyclic Tetramer: Ligand Isomerism of S₂O₂ Macrocycles During the Assembly of Supramolecular Silver(I) Complexes. *Eur. J. Inorg. Chem.* **2006**, *2006*, 3525–3531. (c) Lee, S. Y.; Lee, S. S. Anion-Directed Supramolecular Silver(I) Complexes of an O₂S₂-Macrocycle: Cyclic Oligomer and 2-D Coordination Polymers. *CrystEngComm* **2010**, *12*, 3471–3475. (d) Park, S.; Lindoy, L. F.; Lee, S. S. Assembly of Silver(I) Complexes of Isomeric NS₂-Macrocycles Displaying Cyclic Oligomer, Helix, and Zigzag Structures. *Cryst. Growth Des.* **2012**, *12*, 1320–1329.
- (6) (a) Lee, H.-H.; Lee, E.; Ju, H.; Kim, S.; Park, I.-H.; Lee, S. S. Influence of Anion and Mole Ratio on the Coordination Behavior of an NO₂S₃-Macrocycle: The Formation of a Dumbbell-Shaped Macrocylic Cadmium(II) Iodide Complex. *Inorg. Chem.* **2016**, *55*, 2634–2640. (b) Lee, H.-H.; Park, I.-H.; Lee, S. S. Cooperative Effect of Anion and Mole Ratio on the Coordination Modes of an NO₂S₃-Donor Macrocycle. *Inorg. Chem.* **2014**, *53*, 4763–4769. (c) Han, M. Y.; Min, K. S.; Suh, M. P. Synthesis and Properties of a Molecular Dumbbell with Bis-μ₄-oxo Copper(II/I) Hepta Metal Centers. *Inorg. Chem.* **1999**, *38*, 4374–4375. (d) Golecki, M.; Kersting, B. Preparation, Properties, and Structures of Pentanuclear {[Ni₂L]₂(μ-salen)M]²⁺ Complexes (L = Macrocylic N₆S₂-Donor Ligand). *Z. Anorg. Allg. Chem.* **2015**, *641*, 436–441.
- (7) (a) Ju, H.; Lee, S. S. Assembly of Soft Metal Complexes of an O₄S₂-Macrocycle Displaying Endocyclic Monomer, Dumbbell-Like Dimer, and Endo-/Exocyclic Polymer Structures. *Cryst. Growth Des.* **2012**, *12*, 4972–4980. (b) Seo, J.; Lee, S. Y.; Lee, S. S. Supramolecular Assembly of Dumbbell-shaped Disilver Complex from Thioxamacrocycle and 4,4'-Bipyridine. *Supramol. Chem.* **2007**, *19*, 333–339. (c) Lee, S. Y.; Park, S.; Seo, J.; Lee, S. S. One-Pot Synthesis of Molecular Dumbbell, [AgL(μ-bpy)AgL]²⁺ (L = S₂O₂-Macrocycle; Bpy = 4,4'-Bipyridine). *Inorg. Chem. Commun.* **2007**, *10*, 1102–1104.
- (8) (a) Janzen, D. E.; Chen, W.; VanDerveer, D. G.; Mehne, L. F.; Grant, G. J. Synthesis and Structural Studies of Ruthenium(II) 12S4 Complexes with 4,4'-Bipyridine: The Crystal Structures of [Ru(12S4)(bpy)Cl](Cl)·H₂O and [{Ru(12S4)Cl]₂-μ-(bpy)](PF₆)₂·2CH₃CN. *Inorg. Chem. Commun.* **2006**, *9*, 992–995. (b) Ray, A.; Mijanuddin, M.; Chatterjee, R.; Marek, J.; Mondal, S.; Ali, M. Synthesis, Crystal Structure and Helical Ladder-Like Assembly of a Novel Terephthalato-Bridged Binuclear Cu(II) Complex: First Report on Terephthalate Bridging under Tetraaza Macrocylic Environment. *Inorg. Chem. Commun.* **2006**, *9*, 167–170. (c) Ou, G.-C.; Li, Z.-Z.; Yuan, L.; Yuan, X.-Y. Synthesis and Crystal Structures of Three Isophthalato-Bridged Macrocylic Nickel(II) Complexes. *J. Chem. Sci.* **2015**, *127*, 115–122.
- (9) Williams, N. J.; Hancock, R. D.; Riebenspies, J. H.; Fernandes, M.; de Sousa, A. S. Complexation of Mercury(I) and Mercury(II) by 18-Crown-6: Hydrothermal Synthesis of the Mercuric Nitrite Complex. *Inorg. Chem.* **2009**, *48*, 11724–11733.
- (10) Malleier, R.; Kopacka, H.; Schuh, W.; Wurst, K.; Peringer, P. ¹J(¹⁹⁹Hg/¹⁹⁹Hg) Values of up to 284 kHz in Complexes of [Hg-Hg]²⁺ with Crown Ethers: The Largest Indirect Coupling Constants. *Chem. Commun.* **2001**, 51–52.
- (11) Kadarkaraisamy, M.; Sykes, A. G. Selective Luminescence Detection of Cadmium(II) and Mercury(II) Utilizing Sulfur-containing Anthraquinone Macrocycles (part 2) and Formation of an Unusual Hg₂²⁺-Crown Ether Dimer via Reduction of Hg(II) by DMF. *Polyhedron* **2007**, *26*, 1323–1330.
- (12) Panda, S.; Singh, H. B.; Butcher, R. J. Synthesis and Structure of Mercurous Ion and Dinuclear Lead(II) Complexes of the 28-Membered Selenaza Macrocycle: Dominance of the Chelate Ring Size Effect and Conformational Requirement over Soft-Soft Interactions. *Inorg. Chem.* **2004**, *43*, 8532–8537.
- (13) (a) Hain, M. S.; Fukuda, Y.; Rojas Ramírez, C.; Winer, B. Y.; Winslow, S. E.; Pike, R. D.; Bebout, D. C. Staging Bonding Between Group 12 Metal Ions and Neutral Selenium Donors: Intermolecular Interactions of Mixed N,Se Donor Ligands and Anions. *Cryst. Growth Des.* **2014**, *14*, 6497–6507. (b) Carra, B. J.; Berry, S. M.; Pike, R. D.; Bebout, D. C. Structure and Isomerization Comparison of Zn(II), Cd(II) and Hg(II) Perchlorate Complexes of 2,6-Bis((2-pyridylmethyl)amino)methylpyridine. *Dalton Trans.* **2013**, *42*, 14424–14431. (c) Carra, B. J.; Till, S. N.; VanGundy, R. A.; Pike, R. D.; Bebout, D. C. Group 12 Complexes of 2,6-Bis((2-pyridinylmethyl)thio)methylpyridine: Synthesis and Characterization by X-ray Crystallography and Proton NMR. *Polyhedron* **2016**, *114*, 278–285.
- (14) (a) Huszthy, P.; Bradshaw, J. S.; Zhu, C. Y.; Izatt, R. M.; Lifson, S. Recognition by New Symmetrically Substituted Chiral Diphenyl- and Di-tert-butylpyridino-18-crown-6 and Asymmetrically Substituted Chiral Dimethylpyridino-18-crown-6 Ligands of the Enantiomers of Various Organic Ammonium Perchlorates. *J. Org. Chem.* **1991**, *56*, 3330–3336. (b) Lee, E.; Park, K.-M.; Ikeda, M.; Kuwahara, S.; Habata, Y.; Lee, S. S. Coordination Networks of a Ditopic Macrocycle Exhibiting Anion-Controlled Dimensional Changes and Crystal-to-Crystal Anion Exchange. *Inorg. Chem.* **2015**, *54*, 5372–5383. (c) Teixidor, F.; Escriche, L.; Casabó, J.; Molins, E.; Miravittles, C. Metal Complexes with Polydentate Sulfur-Containing Ligands. Crystal Structure of (2,6-Bis((ethylthio)methyl)pyridine)dibromozinc(II). *Inorg. Chem.* **1986**, *25*, 4060–4062. (d) Bradshaw, J. S.; Huszthy, P.; McDaniel, C. W.; Zhu, C. Y.; Dalley, N. K.; Izatt, R. M.; Lifson, S. Enantiomeric Recognition of Organic Ammonium Salts by Chiral Dialkyl-, Dialkyl-, and Tetramethyl-Substituted Pyridino-18-crown-6

and Tetramethyl-Substituted Bispyridino-18-crown-6 Ligands: Comparison of Temperature-dependent Proton NMR and Empirical Force Field Techniques. *J. Org. Chem.* **1990**, *55*, 3129–3137.

(15) (a) Jung, D.; Chamura, R.; Habata, Y.; Lee, S. S. Extra Large Macrocycle: 40-Membered Macrocycle via 2:2 Cyclization and Its Dimercury(II) Complex. *Inorg. Chem.* **2011**, *50*, 8392–8396. (b) Lee, S.-G.; Park, K.-M.; Habata, Y.; Lee, S. S. Endo- and Exocyclic Supramolecular Complexes of Mixed-Donor Macrocycles via [1:1] and [2:2] Cyclizations. *Inorg. Chem.* **2013**, *52*, 8416–8426. (c) Habata, Y.; Seo, J.; Otawa, S.; Osaka, F.; Noto, K.; Lee, S. S. Synthesis of Diazahexathia-24-crown-8 Derivatives and Structures of Ag⁺ Complexes. *Dalton Trans.* **2006**, 2202–2206.

(16) Kim, H.-S.; Kwon, I.-C.; Choi, J.-H. Synthesis of Crown Ethers Containing a Thiazole Subcyclic Unit. *J. Heterocycl. Chem.* **1999**, *36*, 1285–1289.

(17) (a) Cameron, S. A.; Brooker, S. Metal-Free and Dicopper(II) Complexes of Schiff Base [2 + 2] Macrocycles Derived from 2,2'-Iminobisbenzaldehyde: Syntheses, Structures, and Electrochemistry. *Inorg. Chem.* **2011**, *50*, 3697–3706. (b) Kim, K.-J.; Jung, D.-S.; Kim, D.-S.; Choi, C.-K.; Park, K.-M.; Byun, J.-C. Synthesis and Characterization of Dinuclear Ni(II) Complexes with Tetraazadiphenol Macrocycle Bearing Cyclohexanes. *Bull. Korean Chem. Soc.* **2006**, *27*, 1747–1751. (c) Brooker, S. Complexes of Thiophenolate-Containing Schiff-Base Macrocycles and Their Amine Analogues. *Coord. Chem. Rev.* **2001**, *222*, 33–56. (d) MacLachlan, M. J.; Park, M. K.; Thompson, L. K. Coordination Compounds of Schiff-Base Ligands Derived from Diaminomaleonitrile (DMN): Mononuclear, Dinuclear, and Macrocyclic Derivatives. *Inorg. Chem.* **1996**, *35*, 5492–5499. (e) Menif, R.; Martell, A. E.; Squattrito, P. J.; Clearfield, A. New Hexaaza Macrocyclic Binucleating Ligands. Oxygen Insertion with a Dicopper(I) Schiff Base Macrocyclic Complex. *Inorg. Chem.* **1990**, *29*, 4723–4729.

(18) Catalano, V. J.; Malwitz, M. A.; Noll, B. C. Pd(0) and Pt(0) Metallocryptands Encapsulating a Spinning Mercurous Dimer. *Inorg. Chem.* **2002**, *41*, 6553–6559.

(19) Bebout, D. C.; Bush, J. F., II; Shumann, E. M.; Viehweg, J. A.; Kastner, M. E.; Parrish, D. A.; Baldwin, S. M. Caging the Mercurous Ion: A Tetradentate Tripodal Nitrogen Ligand Enhances Stability and *J*(¹H¹⁹⁹Hg). *J. Chem. Crystallogr.* **2003**, *33*, 457–463.

(20) (a) Argent, S. P.; Adams, H.; Riis-Johannessen, T.; Jeffery, J. C.; Harding, L. P.; Clegg, W.; Harrington, R. W.; Ward, M. D. Complexes of Ag(I), Hg(I) and Hg(II) with Multidentate Pyrazolyl-Pyridine Ligands: From Mononuclear Complexes to Coordination Polymers via Helicates, a Mesocate, a Cage and a Catenate. *Dalton Trans.* **2006**, *42*, 4996–5013. (b) Kepert, D. L.; Taylor, D.; White, A. H. Crystal Structure of 4-Cyanopyridinemercury(I) Perchlorate. *Inorg. Chem.* **1972**, *11*, 1639–1643. (c) Meyer, G.; Jurkiewicz, I.; Nolte, M.; Mudring, A.-V. Strong Attraction of Caffeine to the Mercurous Dumbbell in the Salt [Hg₂(Caf)₂](ClO₄)₂(H₂O)₂. *Z. Anorg. Allg. Chem.* **2004**, *630*, 1933–1936. (d) Malleier, R.; Schuh, W.; Kopacka, H.; Wurst, K.; Peringer, P. [Hg₂]²⁺ Coordinated by Eight Nitrogen Donor Atoms: Synthesis and Structure of [Hg₂(phen)₄](OTf)₂, Phen = 1,10-Phenanthroline. *Inorg. Chim. Acta* **2008**, *361*, 195–198. (e) Li, Y.; Zhang, J.-A.; Wang, Y.-B.; Pan, M.; Su, C.-Y. Crystal Structures, DFT Calculations and Biological Activities of Three Mercury Complexes from a Pentadentate Thioether Ligand. *Inorg. Chem. Commun.* **2013**, *34*, 4–7. (f) Kepert, D. L.; Taylor, D.; White, A. H. Crystal Structure of Bis[(3-chloropyridine)mercury(I)] Dipperchlorate. *J. Chem. Soc., Dalton Trans.* **1973**, *8*, 893–896. (g) Dewan, J. C.; Kepert, D. L.; White, A. H. Crystal Structure of Bis-[(1,8-naphthyridine)mercury(I)] Dipperchlorate. *J. Chem. Soc., Dalton Trans.* **1975**, *6*, 490–492. (h) Kepert, D. L.; Taylor, D.; White, A. H. Crystal Structure of Hexakis(triphenylphosphine oxide)dimercury(I) Bisperchlorate. *J. Chem. Soc., Dalton Trans.* **1973**, *16*, 1658–1662. (i) Elder, R. C.; Halpern, J.; Pond, J. S. The Preparation and Crystal Structure of 1,10-Phenanthroline-mercury(I) Nitrate, Hg₂(phen)(NO₃)₂. *J. Am. Chem. Soc.* **1967**, *89*, 6877–6880. (j) Kepert, D. L.; Taylor, D.; White, A. Crystal Structure of the Dimeric Pyridine 1-Oxide Complex with Mercury(I) Perchlorate. *J. Chem. Soc., Dalton*

Trans. **1973**, *50*, 392–396. (k) Xu, F.; Peng, Y.-X.; Hu, B.; Tao, T.; Huang, W. Comparative Structural and Spectral Analyses for Mononuclear and Dinuclear Metal Complexes of 2-Thiophen and 2-(5-Bromothiophen) Imidazo[4,5-f][1,10]phenanthroline. *CrystEngComm* **2012**, *14*, 8023–8032. (l) Brodersen, K.; Hofmann, J. Synthese und Kristallstruktur von Bis(m-aminobenzonitril)-diquecksilber(I)-dinitrat. *Z. Naturforsch., B: J. Chem. Sci.* **1992**, *47*, 460–464. (m) Brodersen, K.; Zimmerhackl, J. Synthese und Kristallstruktur von 1,13-Bis(8-chinoly)l-1,4,7,10,13-pentaoxatridecan-diquecksilber(I)-diperchlorat. *Z. Naturforsch., B: J. Chem. Sci.* **1991**, *46*, 1–4.

(21) Lee, E.; Lee, S. S. Syntheses and Crystal Structures of Mercury(II) and Copper(II) Complexes of an 18-Membered NS₄-Macrocycle. *Bull. Korean Chem. Soc.* **2015**, *36*, 36–42.

(22) Kang, G.-C.; Park, I.-H.; Lee, S. S. An Unusual Pseudo-Coordination Polymer of Dithia-18-crown-6 with Heavy Metal. *Bull. Korean Chem. Soc.* **2012**, *33*, 3875–3878.

(23) APEX 2 and SAINT: Area Detector Control and Integration Software, version 6.22; Bruker AXS Inc.; Madison, WI, 2000.

(24) SHELXTL: Program for Solution and Refinement of Crystal Structures, version 6.10; Bruker AXS Inc.: Madison, WI, 2000.